

# A Molecular Einstein Ring: Imaging a Starburst Disk Surrounding a Quasi-Stellar Object

C. L. Carilli

National Radio Astronomy Observatory, P.O. Box O, Socorro, NM, 87801, USA  
ccarilli@nrao.edu

G.F. Lewis

School of Physics, University of Sydney, NSW 2006, Australia

S.G. Djorgovski & A. Mahabal

Astronomy Department, California Institute of Technology, Pasadena, CA, 91125, USA

P. Cox

Institut d'Astrophysique Spatiale, Université de Paris XI, 91405 Orsay, France

F. Bertoldi

Max-planck Institut für Radioastronomie, Auf dem Hügel 69, Bonn, D-53121, Germany

A. Omont

Institut d'Astrophysique de Paris, CNRS, 98 bis boulevard Arago, F-75014, Paris, France

Images of the CO 2–1 line emission, and the radio continuum emission, from the redshift 4.12 gravitationally lensed quasi-stellar object (QSO) PSS J2322+1944 reveal an Einstein ring with a diameter of  $1.5''$ . These observations are modeled as a star forming disk surrounding the QSO nucleus with a radius of 2 kpc. The implied massive star formation rate is  $900 M_{\odot} \text{ year}^{-1}$ . At this rate a substantial fraction of the stars in a large elliptical galaxy could form on a dynamical time scale of  $10^8$  years. The observation of active star formation in the host galaxy of a high-redshift QSO supports the hypothesis of coeval formation of supermassive black holes and stars in spheroidal galaxies.

Establishing a link between galaxy formation and massive black hole formation has become paramount for observational astronomy since the discovery of the correlation between black hole mass and stellar bulge mass in nearby ( $z < 0.1$ ) galaxies (1). This correlation suggests a ‘causal connection between the formation and evolution of the black hole and the bulge’ (2), and has led to the hypothesis of co-eval formation at high redshift ( $z > 2$ ) of massive black holes and spheroidal galaxies (3,4,5). Supermassive black holes ( $\geq 10^9 M_\odot$ ) at high redshift manifest themselves as optically luminous quasi-stellar objects (QSOs) powered by mass accretion onto the hole.

Observations of high redshift QSOs have shown that 30% are luminous infrared sources, with far infrared (FIR) luminosities  $\sim 10^{13} L_\odot$ , corresponding to thermal emission from warm dust (6-9). The key question for these FIR luminous QSOs is: what is the dominant dust heating mechanism, star formation or the active galactic nucleus (AGN)? If the dust is heated by star formation, the star formation rates must be of order  $10^3 M_\odot \text{ year}^{-1}$ , supporting the idea of co-eval formation of the stars and black holes in these systems. Molecular (CO) line emission has been detected from a number of these FIR-luminous high redshift QSOs, implying large reservoirs of molecular gas ( $> 10^{10} M_\odot$ ), suggesting that star formation may be inevitable (9). However, in most cases the FIR luminosity corresponds to only 10% of the bolometric luminosity of the system, and hence the case for co-eval star formation and mass accretion onto a supermassive black hole at high redshift remains circumstantial.

The QSO PSS 2322+1944 at  $z = 4.12$  is among the most IR-luminous high redshift QSOs, with an apparent FIR luminosity of  $3 \times 10^{13} L_\odot$  (11). Optical imaging and spectroscopy shows that 2322+1944 is a double source, with two essentially identical spectrum components separated by about  $1.5''$  (10), indicating strong gravitational lensing by an intervening galaxy. PSS 2322+1944 is also the brightest known CO line emitting source at  $z > 4$ , with an implied molecular gas mass of  $2 \times 10^{11} M_\odot$  (11) (not corrected for lens magnification). Non-thermal (synchrotron) radio continuum emission from 2322+1944 was detected at 1.4 GHz, and the rest frame radio-through-IR spectral energy distribution of 2322+1944 matches closely that of the prototype nuclear starburst galaxy M82 (7,11). Overall, the properties of PSS2322+1944 make it the best candidate for very active star formation in the host galaxy of a high redshift QSO. In this paper we present high resolution imaging of the CO and radio continuum emission from PSS 2322+1944 which address this interesting possibility.

We have observed the CO 2–1 emission from the PSS 2322+1944 at a resolution of  $0.6''$  using the Very Large Array (VLA). The velocity-integrated CO emission from PSS 2322+1944 (Fig. 1) forms a

complete ring with a diameter of about  $1.5''$ . We interpret this structure as an ‘Einstein ring’ resulting from strong gravitational lensing. The individual velocity channel images (Fig. 2) show that the CO emission shifts position with velocity, with the peak surface brightness moving by about  $1''$  from the southeast at low velocity, to the north at high velocities. We have also reanalyzed the 1.4 GHz VLA radio continuum observations of PSS 2322+1944 of (7) by using different weighting of the visibility data in order to optimize spatial resolution, as opposed to the previous analysis which optimized sensitivity at the expense of resolution (Fig. 3). At this improved resolution ( $1.1''$ ), it is clear that the 1.4 GHz emission forms a structure similar in size and shape to that seen in the CO emission.

The unknown characteristics of the lensing galaxy toward 2322+1944 do not warrant a detailed gravitational lensing inversion. Einstein rings, however, are generic features of gravitational lens models (12, 13) and hence we adopt a typical gravitational lens model in our analysis. In particular, we adopt a lens potential of the form found for the strongly lensed radio galaxy MG 1131+0456 by (14), including a mass distribution with an ellipticity of 0.15 at an angle of  $36^\circ$ , and a central velocity dispersion of  $230 \text{ km s}^{-1}$ . By examining various source configurations, and by considering the individual channel maps, the observed ring structure is reconstructed (Fig. 4).

In this model the optical QSO is located between the inner and outer caustics for the lens (Figure 4) and is imaged into two point sources with a total magnification of  $\sim 3.5$ . The observed CO Einstein ring can be reproduced by a molecular gas distribution corresponding to an inclined disk surrounding the optical QSO. Such disks are characteristic of the molecular gas and dust distribution in IR-luminous galaxies seen at low redshift (15). To form the observed Einstein ring structure, the CO emission must extend south of the QSO by at least  $\sim 0.3''$  in the source plane, corresponding to  $\sim 2.2 \text{ kpc}$  assuming a concordance cosmology ( $H_o = 65 \text{ km s}^{-1} \text{ Mpc}^{-1}$ ,  $\Omega_M = 0.3$  and  $\Omega_\Lambda = 0.7$ ), crossing a significant fraction of the inner caustic (16). The scale of the caustic structure relative to the critical lines is typical of lens models and hence the lensing mass distribution would have to be pathologically different to other lens systems to significantly modify this conclusion. The total magnification factor for the CO emission is  $\sim 2.5$ , but this number is dependent upon the thickness of the CO disk (or inclination angle), as thinner disks will be more strongly magnified. The CO component on the northern side of the QSO (away from the inner caustic) crosses the outer caustic. This outer component forms two features in the image plane. The magnification for this northern component is less than that for the southern component by a factor of 2.5 in this model. This model reproduces the basic features of the observed structures, including the relative locations and separations of the double optical QSO and the CO Einstein ring, and the positions and relative strengths

of the three peaks in the CO distribution (Fig. 1).

The CO emission presents different structure at different velocities (Fig. 2) consistent with the source straddling the central diamond caustic. We have considered the source plane distribution of CO as a function of velocity using the lens model above, and find that the results are consistent with a disk with a velocity gradient of  $115 \text{ km s}^{-1} \text{ kpc}^{-1}$ , implying a mass enclosed within 2.2 kpc of  $3 \times 10^{10} \times \sin^{-2} i M_{\odot}$ , where  $i$  is the disk inclination angle with respect to the plane of the sky. The center of the lensing galaxy should lie close to that of the CO ring, roughly 0.5 arcseconds north of the southern QSO image. Assuming a (likely) lens redshift of  $z \sim 1$ , its inferred velocity dispersion is  $\sim 230 \text{ km s}^{-1}$ , suggesting gravitational lensing by a single galaxy. Hence PSS 2322+1944 represents a prime candidate for a 'Golden Lens' (17) from which Hubble's constant can be determined via the measurement of the time delay between the quasar images.

An additional critical constraint on the physical interpretation of this system is that the observed radio continuum morphology is similar to that of the CO emission, implying similar source plane distributions. While the CO and radio continuum emission form similar rings in the image plane, the radio continuum peak surface brightness is shifted by  $0.37'' \pm 0.3''$  from the CO peak, where the positional error is based on the signal-to-noise ratio of the peak in the 1.4 GHz image. Hence the position offset could be due to noise, or it could reflect real source-plane differences on sub-kpc scales between the radio continuum and CO emission.

The ability of this simplistic modeling approach to recreate the observed CO configuration highlights the generic nature of Einstein rings in elliptical gravitational lenses. Most importantly, our physical interpretation of this system below relies on the two most robust aspects of these observations and modeling: (i) the relative extent of the CO source with respect to the optical QSO in the source plane, and (ii) the rough co-spatiality of the CO and radio continuum emission.

The telescopic effect of strong lensing provides the unique opportunity to study the sub-kpc scale structure in the parent galaxy of this system, and these results have direct relevance to the critical question of whether the dust in high redshift, FIR-luminous QSOs is heated directly by the AGN or by star formation. For PSS 2322+1944 the relative image plane distribution of the optical and CO emission implies that the strongly magnified CO emitting regions must be spatially separated from the QSO by about 2 kpc. The data are consistent with a model in which the molecular gas is in an inclined disk surrounding the QSO. Although high resolution imaging of the thermal dust continuum emission from PSS 2322+1944 has

not been performed, it is reasonable to assume that the molecular gas and dust are roughly co-spatial (18).

Dust heating on kpc-scales has long been considered a problem for point-source (ie. AGN) heating models, especially for disk-like dust distributions (15). The primary difficulty is self-shielding and the (lack of) illumination of an extended disk by an obscured central source. Possible solutions to this problem include warped disks (19), and heating by dust-penetrating soft X-rays (20).

For PSS 2322+1944 we have also found that the radio continuum emission is roughly co-spatial with the molecular gas, and not with the optical QSO. This morphology is not what is expected for radio emission from the AGN itself. Non-thermal radio emission directly associated with supermassive black holes invariably takes the form of a core-jet radio source, with the dominant radio emission coming from high energy electrons accelerated in strong shocks in highly collimated relativistic outflows from the supermassive black hole (21). In this case the observed radio morphology would more closely resemble that of the optical QSO, ie. a double radio source coincident with the optical QSOs, and perhaps with extensions corresponding to a jet.

The fact that the radio continuum emitting material is co-spatial with the molecular gas, and presumably the dust, in PSS 2322+1944 is exactly what is expected for a star forming galaxy. The molecular gas, dust, and radio continuum emission are always well correlated on kpc scales in star forming galaxies (18), originating in regions of active star formation. Given the requisite large gas mass to fuel star formation, and the similarity of the radio-to-IR SED of PSS 2322+1944 to that of a star forming galaxy, we conclude that the QSO in PSS 2322+1944 is surrounded by a starburst disk on a scale of 2 kpc. These observations provide the most direct evidence to date of active star formation in the host galaxy of a luminous, high redshift QSO. The implied massive star formation rate is  $\sim 900 M_{\odot} \text{ year}^{-1}$  based on the thermal IR luminosity. At this rate a substantial fraction of the stars in a large elliptical galaxy could form on a dynamical timescale of  $\leq 10^8$  years.

## REFERENCES

- 1 Ferrarese, L. & Merritt, D. 2000, *ApJ* (letters), 539, 9
- 2 Gebhardt, Karl et al. 2000, *ApJ* (letters), 539, 13
- 3 Blain, A.W. Jameson, A., Smail, I., Longair, M.S., Kneib, J.-P., & Ivison, R.J. 1999, *MNRAS*, 309, 715
- 4 Kauffmann, G. & Haehnelt, M. 2000, *MNRAS*, 311, 576
- 5 Page, M.J., Stevens, J.A., Mittaz, J., Carrera, F.J. 2001, *Science*, 294, 2516
- 6 Carilli, C.L., Bertoldi, F., Rupen, M.P. et al. 2001a, *ApJ*, 555, 625
- 7 Carilli, C.L., Bertoldi, F., Omont, A., Cox, P., McMahon, R.G., & Isaak, K. 2001b, *AJ*, 122, 1679
- 8 Carilli, C.L., Cox, P., Bertoldi, F. et al. 2002, *ApJ*, 575, 145
- 9 Omont, A., Cox, P.; Bertoldi, F., McMahon, R. G., Carilli, C., & Isaak, K. G 2001, *A& A*, 374, 371
- 10 Djorgovski, S.G., A. Mahabal, et al. 2003, *ApJ*, in prep
- 11 Cox, P., Omont, A., Djorgovski, G., Bertoldi, F. et al. 2002, *A & A*, 387, 406
- 12 Kochanek C. S., Keeton C. R., McLeod B. A., 2001, *ApJ*, 547, 50
- 13 Saha P., Williams L. L., 2001, *AJ*, 122, 585
- 14 Kochanek, C.S., Blandford, R.D., Lawrence, C.R., Narayan, R. 1989, *MNRAS*, 238, 43
- 15 Downes, D., & Solomon, P.M. 1998, *ApJ*, 507, 615
- 16 In gravitational lensing, caustics represent the locations in the source plane of infinite magnification, and the critical lines are the locations of the corresponding structures in the image plane.
- 17 Williams, L.L., Schechter, P.L. 1997, *Astron. & Geo.*, 38, 10
- 18 Adler, D., Lo, K.Y., & Allen, R. 1991, *ApJ*, 382, 475
- 19 Sanders, D.B., Phinney, E. S., Neugebauer, G., Soifer, B. T., & Matthews, K. 1989, *ApJ*, 347, 29
- 20 Maloney, P.R. 1999, *Ap&SS* 266, 207
- 21 Begelman, M. Blandford, R., Rees, M. 1984, *Rev. Mod. Phys.*, 56, 255
- 22 The National Radio Astronomy Observatory (NRAO) is operated by Associated Universities, Inc. under a cooperative agreement with the National Science Foundation. SDG acknowledges partial support from

the Bressler Foundation.

### Figure Captions

FIG. 1.— The contour image of the total CO 2–1 emission (rest frame frequency = 230.538 GHz) from PSS 2322+1944 made from observations with the Very Large Array (VLA). Observations were made in October and November, 2002 in the C configuration (max. baseline = 3 km), giving a resolution of  $0.6''$  at the central observing frequency of 45.035 GHz. The total observing time was 18 hours. Fast switching phase calibration was employed (150 sec total calibration cycle time), and phase coherence was monitored using test cycles on nearby calibrators. At all times the coherence was found to be better than 85%. The root-mean-square (rms) noise on this image is  $0.09 \text{ mJy beam}^{-1}$ . The contour levels are a geometric progression in square root two starting at  $0.12 \text{ mJy beam}^{-1}$ . The Gaussian restoring CLEAN beam has  $\text{FWHM} = 0.63'' \times 0.55''$  with a major axis position angle of  $-30^\circ$ . The crosses show the positions of the optical QSOs, and the cross sizes represent the relative astrometric error (10).

FIG. 2. — The spectral channel images of the CO 2–1 emission from PSS 2322+1944. Seven spectral channels were used with a channel width of 6.25 MHz (42 km/s), and the center of channel 4 was at 45.035 GHz ( $z = 4.1191$  for CO 2–1). Low spatial resolution imaging of CO 1–0 emission from PSS 2322+1944 constrains the line center to be at  $z = 4.1192 \pm 0.0004$ , and the line  $\text{FWHM} = 280 \text{ km s}^{-1}$  (8). Image cubes were synthesized using natural weighting of the visibilities, and the final image cube was Hanning smoothed such that adjacent channels are not independent. The rms noise per Hanning smoothed channel was  $0.13 \text{ mJy beam}^{-1}$ . Channel 7 was found to have higher noise than the other channels, and was removed from the image cube before Hanning smoothing. The contour scheme is the same as Figure 1, starting at  $0.25 \text{ mJy beam}^{-1}$ . The peak surface brightness in the cube is  $0.87 \text{ mJy}$ , corresponding to an observed brightness temperature of 1.4 K.

FIG. 3. — The radio continuum image of PSS 2322+1944 at 1.4 GHz. The rms in this image is  $15 \mu\text{Jy beam}^{-1}$  and the Gaussian restoring beam is circular with  $\text{FWHM} = 1.1''$ . The contour scheme is the same as Figure 1, starting at  $0.02 \text{ mJy beam}^{-1}$ . The total flux density is  $0.12 \text{ mJy}$  and the peak surface brightness is  $56 \mu\text{Jy beam}^{-1}$ .

FIG. 4. — A gravitational lens model for the CO emission in PSS 2322+1944. The model is based on the elliptical lens toward MG 1131+0456 (14). The left hand panel presents the source plane distribution, corresponding to the true (ie. undistorted by lensing) morphology of the system. The image plane distribution is presented in the right hand panel, corresponding to the observed morphology after being distorted by the gravitational lens. The point-like QSO is represented by a five-point star in both panels.

The solid lines are the caustics and critical lines in the source and image planes, respectively (16). The CO emission is modeled as an inclined disk ( $i \sim 60^\circ$ ) around the QSO, with the north and south parts of the disk being color-coded red and blue, respectively, corresponding to different velocity regions on opposite sides of the QSO.

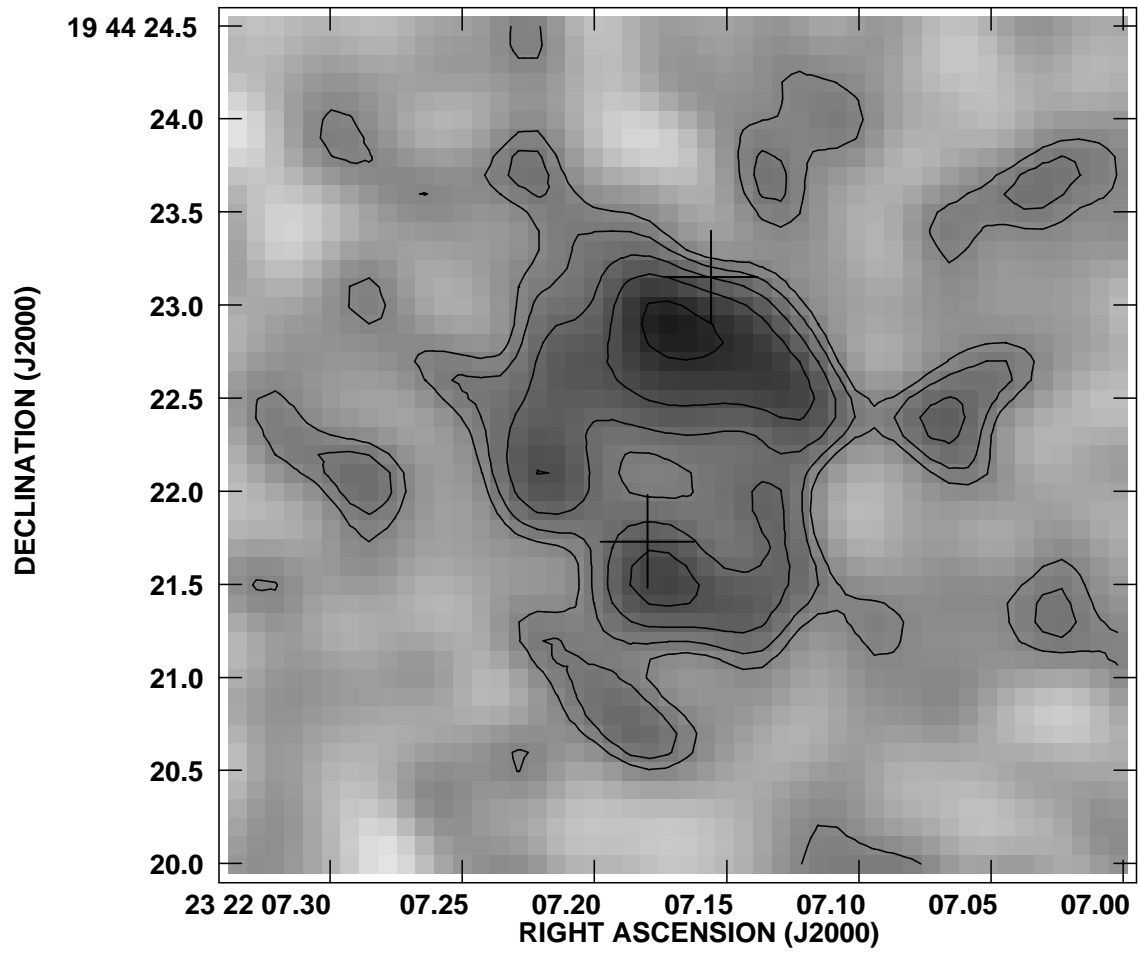


Fig. 1.—

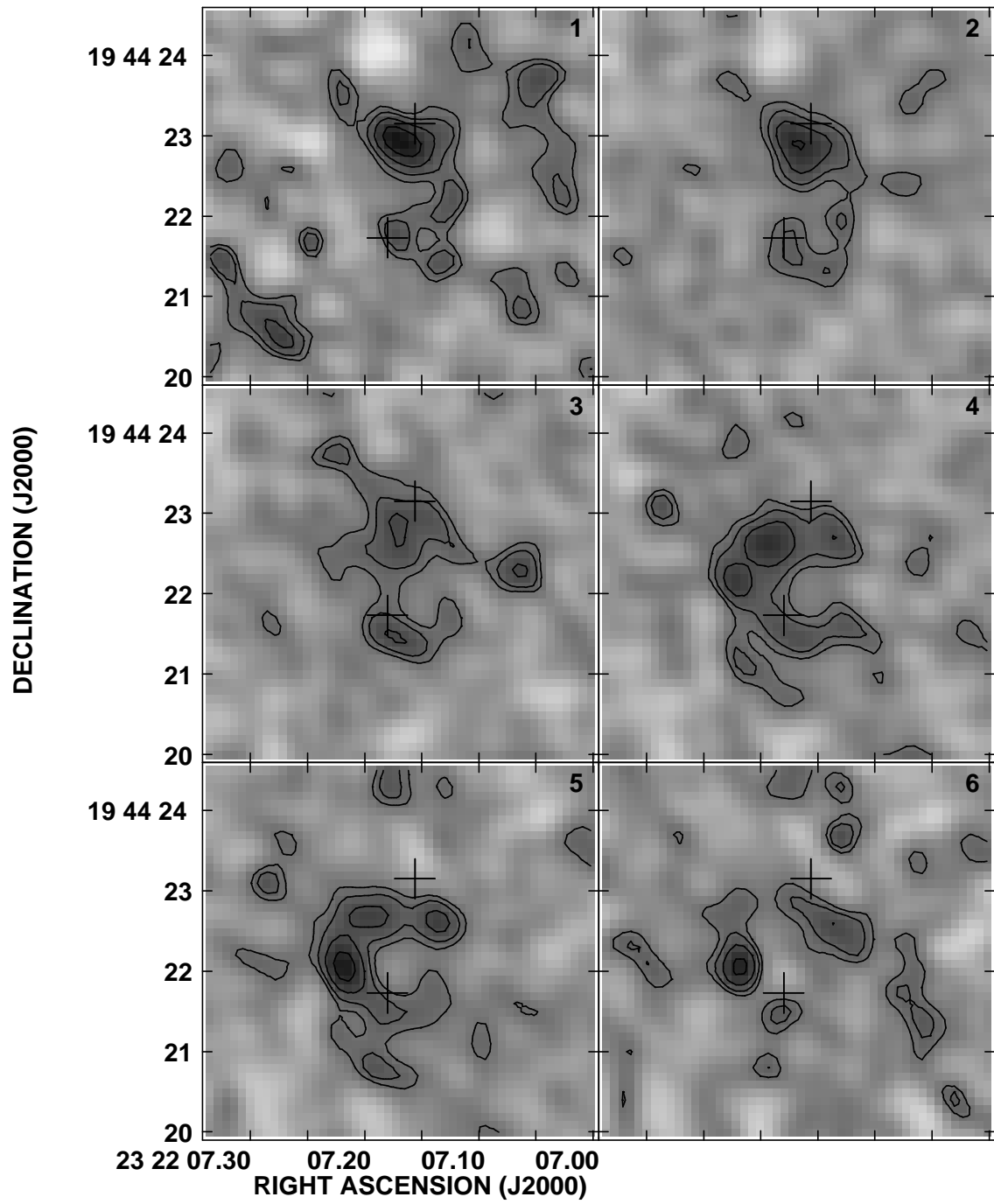


Fig. 2.—

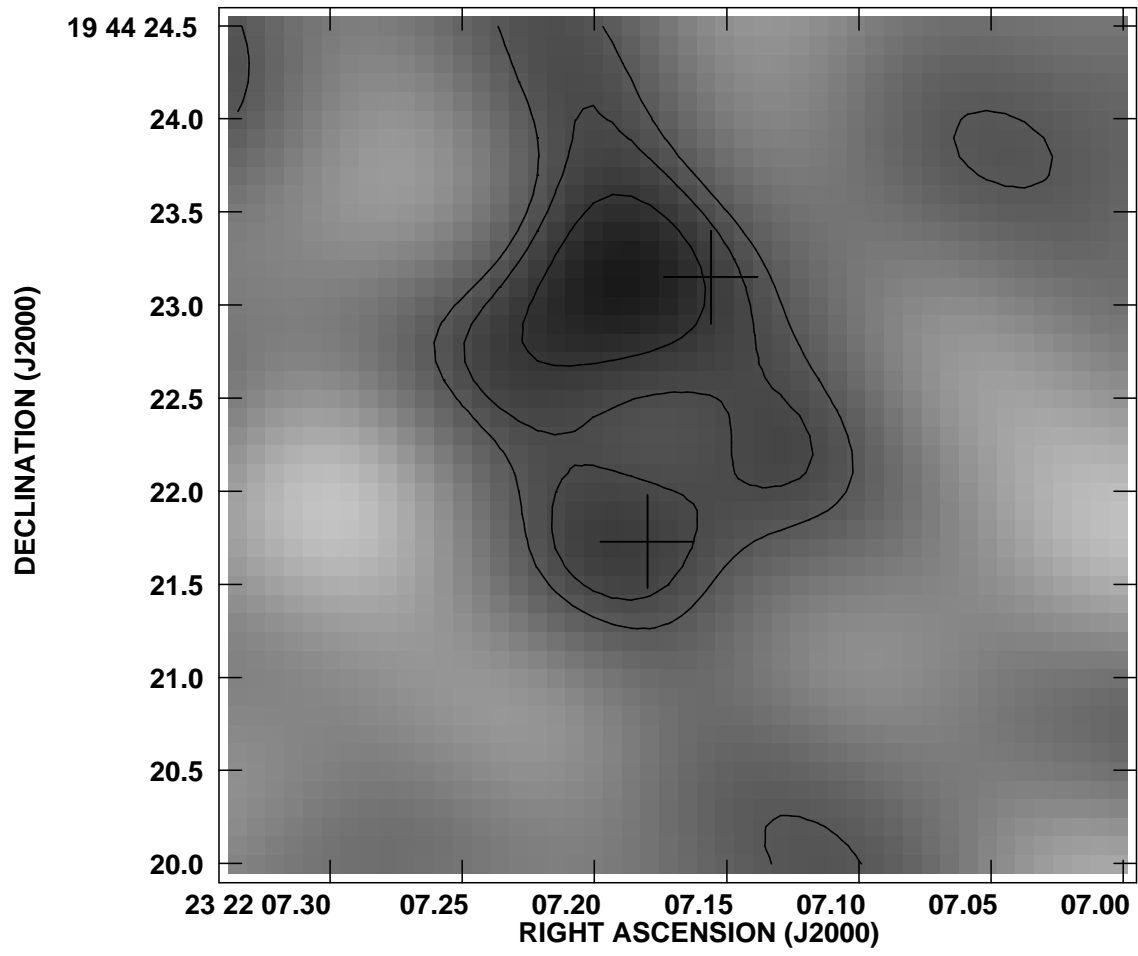


Fig. 3.—

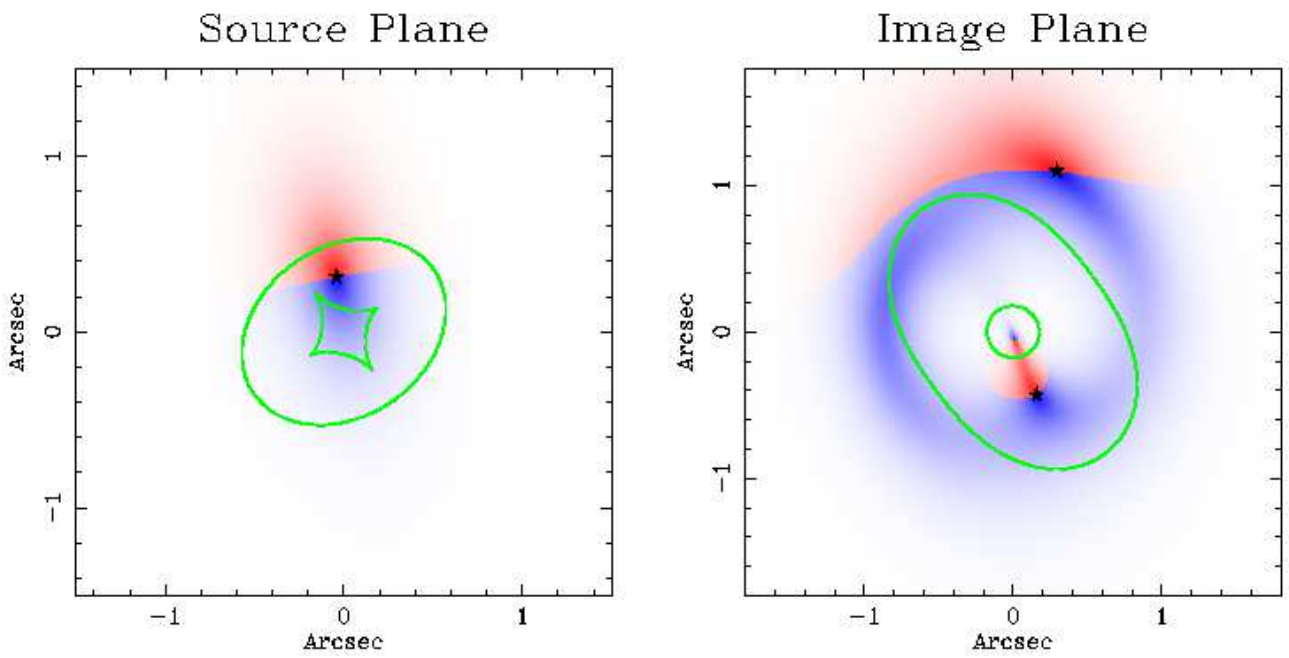


Fig. 4.—